Channel Precoding With Small Envelope Variations for $\pi/4$-QPSK and MSK Over Frequency-Selective Slow Fading Channels

Jennifer S. Y. Lee and Weihua Zhuang, *Senior Member, IEEE*

***Abstract*—This paper presents channel precoding schemes to combat intersymbol interference (ISI) over a frequency-selective slow fading channel in wireless communication systems using $\pi/4$ shifted quadrature phase-shift keying or minimum shift keying. Based on the dimension partitioning technique, the precoders predistort the phase of the transmitted symbol in the forward link to combat ISI, keeping the transmitted symbol amplitude constant. The proposed schemes can ensure the stability of the precoder even in equalizing a nonminimum-phase channel, combat ISI without increasing the complexity of portable unit receivers, and reduce the envelope variations of transmitted signals such that power-efficient nonlinear amplifiers can be used for the precoded signals without causing a significant undue distortion. Theoretical analysis and simulation results are presented to demonstrate the effectiveness of the proposed channel precoding schemes.**

***Index Terms*—Channel precoding, equalization, intersymbol interference (ISI), minimum shift keying (MSK), $\pi/4$ shifted quadrature phase-shift keying ($\pi/4$-QPSK), slow frequency-selective fading.**

I. Introduction

In A wireless communication system, transmitted signals often arrive at the receiver through more than one path, due to reflection, refraction, and scattering of the radio waves, a phenomenon known as multipath fading. Transmitted signals passing through a multipath fading channel suffer from amplitude fluctuation, phase distortion, and propagation delay spread. In high-bit-rate transmission, the delay spread of the channel can be larger than the transmitted symbol interval. This results in intersymbol interference (ISI), which dramatically degrades transmission performance [1], [2]. Channel equalization is widely used to mitigate the effect of ISI [3], [4]. Decision-feedback equalizer (DFE) is the most popular nonlinear equalizer. However, DFE has an inherent error propagation problem. Also, when coded modulation is used to further improve transmission performance, the combination of the Viterbi decoder with a DFE is not straightforward if decoded decisions or tentative decisions are to be used in the DFE. This is because DFE requires delay-free decisions for feedback and, in a coded system, such decisions are not sufficiently reliable. The problem can be solved at the expense of the receiver complexity, such as by using parallel decision feedback decoding (PDFD) [5] and decision-feedback noise prediction with interleaving (DFNPI) [6]. In a wireless system, the complexity constraint of the battery-powered portable unit is more stringent than that of the base station, as the availability of compact, light, handheld portable units is vital. Thus, the PDFD and DFNPI schemes can be used in the reverse link but are not desirable for use in the forward link where the receiver is the portable unit.

One way to maintain the low complexity of the portable unit is to move channel equalization functions in the forward link from the portable unit receiver to the base-station transmitter [7]. This technique is called precoding or preequalization. Channel precoding was originally proposed for time-invariant channels such as a subscriber loop. As wireless mobile channels are in general time-varying, in order to apply channel precoding techniques to a wireless mobile system, certain mechanisms should be in place to ensure that the channel time-varying components (such as the Doppler effect) are accurately tracked and compensated. Consider the time-division duplex (TDD) operation, where the forward link and the reverse link of a duplex channel transmit alternately on the same frequency band. For slow fading channels, under the assumption that the channel characteristics are approximately time-invariant within the duration of one data frame, the estimated channel characteristics of the reverse link obtained at the base-station receiver can be used for the forward link transmission. A precoder at the base-station transmitter can use the available channel information to preequalize the signal to counter the ISI effect. The precoding technique can achieve both portable unit simplicity and ISI reduction. Moreover, powerful coded modulation techniques with Viterbi decoding can be combined easily with the precoding to further improve the system performance [8], [9]. Theoretically, a linear precoder with a transfer function equal to the inverse of the channel transfer function can be used. However, when the fading channel is not minimum phase, the linear precoder becomes unstable. Several nonlinear precoding schemes [10]–[14] have been developed to ensure the stability. Each of the precoding schemes is proposed for a particular modulation scheme. Tomlinson–Harashima (TH) precoding [10], [11] is a classical nonlinear precoding technique for pulse amplitude modulation (PAM) over a band-limited additive white Gaussian noise (AWGN) channel. A precoding scheme using dimension partitioning is proposed in [14] for quadrature phase-shift keying (QPSK) over a wireless fading dispersive channel. The precoder predistorts only the transmitted

Manuscript received July 25, 2000; revised June 21, 2001. This work was supported by the Natural Sciences and Engineering Research Council of Canada under Research Grant OGP0155131 and by the Ontario Government under an Ontario Graduate Scholarship.

J. S. Y. Lee is with Kaval Wireless Technologies Inc., Markham, L3R 8X7 ON, Canada (e-mail: jlee@kaval.com).

W. Zhuang is with the Department of Electrical and Computer Engineering, University of Waterloo, Waterloo, N2L 3G1 ON, Canada (e-mail: wzhuang@bbcr.uwaterloo.ca).

Digital Object Identifier 10.1109/TVT.2002.807226

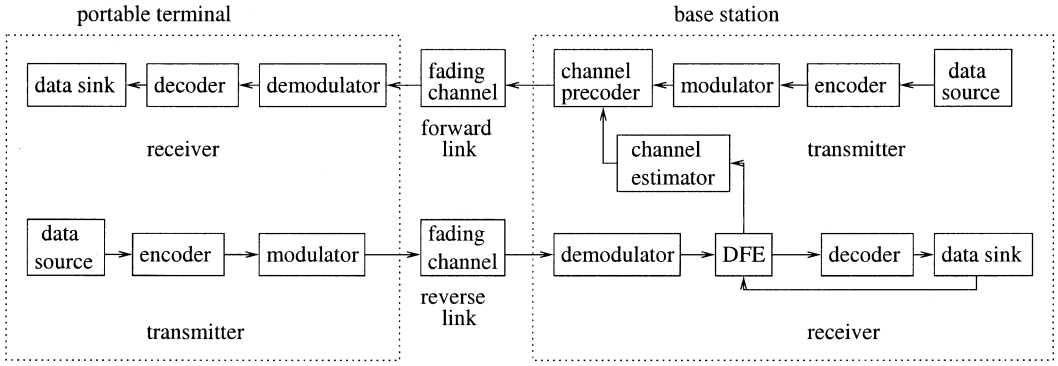

Fig. 1. A functional block diagram of the precoding system.

symbol phase and keeps a constant transmitted symbol amplitude. Precoding for removing ISI introduced by pulse-shaping filters has also been investigated [15], [16]. In this paper, the discrete information-bearing symbol (at baseband) representing the modulated signal over each symbol interval at passband before the transmitter filtering is referred to as *transmitted symbol*, and the modulated signal at passband after the transmitter filtering is referred to as *transmitted signal*.

In wireless communications, in order to meet specified out-of-band spectral emission requirements, signals are bandpass filtered at the transmitters prior to transmission. A widely used bandpass filter is the raised cosine filter. In the North America digital cellular systems (IS-54) [17], a raised cosine filter is split into two square-root raised cosine filters: one for the transmitter and one for the receiver. After filtering, the side lobes of the transmitted signals are suppressed and the band-limited signals will no longer have a constant envelope. When a power-efficient nonlinear amplifier (e.g., class C) is used to amplify the transmitted signal, the nonlinearity of the transmitter power amplifier tends to spread the signal frequency spectrum and hence decreases the spectrum efficiency. The degradation increases for a scheme with a larger signal envelope dynamic range. As a result, modulation schemes with small envelope variations are desired for wireless communications [18]. For example, PSK with small envelope variations such as $\pi/4$ shifted QPSK ($\pi/4$-QPSK) or MSK with constant envelope is preferred to amplitude modulation such as QAM. On the other hand, TH precoding is not suitable for wireless transmission, as it introduces significant amplitude variations to the transmitted signal. Keeping precoded symbol amplitude constant is one way to reduce transmitted signal envelope variations, as in the precoding for QPSK proposed in [14]. However, the QPSK precoding does not eliminate any occasional phase shifts of $\pm\pi$ rad that contribute to large transmitted signal envelope variations after filtering. The envelope variations degrade the spectrum efficiency when the precoded signal is amplified by a nonlinear amplifier.

In this paper, we investigate channel precoding with small envelope variations for $\pi/4$-QPSK and MSK. The newly proposed precoding techniques maintain a constant transmitted symbol amplitude and eliminate abrupt phase shifts of $\pm\pi$ rad to achieve better output spectral characteristics and to allow the use of a power-efficient nonlinear amplifier without an undue distortion. The performance of the precoding techniques is analyzed mathematically and by computer simulations. Numerical results demonstrate that the proposed channel precoders are effective in combating ISI, and the precoding scheme for $\pi/4$-QPSK can achieve a smaller envelope variation than the standard $\pi/4$-QPSK.

This paper is organized as follows. Section II describes the communication system model where the proposed precoding schemes are used. In Section III, the principles and operations of the newly proposed channel precoding techniques are presented. The transmission performance of the system using the proposed precoding techniques is analyzed theoretically in Section IV. Numerical analysis results and computer simulation results of the transmission performance are presented and discussed in Section V. Section VI gives the conclusions of this research.

II. System Description

Fig. 1 shows the functional block diagram of the wireless communication system under consideration. For simplicity, it shows only one base station and one portable unit linked by a wireless channel. This system uses time-division multiple access (TDMA) in TDD with asymmetric channel equalization. The modulation scheme is $\pi/4$-QPSK or MSK. In multiple access, users share the allocated radio spectrum in the time domain. Time is partitioned into data frames, and each frame consists of a number of time slots. With TDD, each user is allocated some slot(s) for the forward link and other slot(s) for the reverse link. Transmissions from various users are interlaced in the frame using the same frequency band. When the transmission rate is high, the fading dispersive channel introduces ISI to the received signal. In the reverse link from the portable unit to the base station, a DFE at the base-station receiver is used to combat the ISI. The channel estimator estimates the channel impulse response based on the tap coefficients of the DFE. For a slow fading channel, the channel characteristics are assumed to be nearly unchanged during one frame. Hence, the estimated channel characteristics in the reverse link can be used in the precoder at the base-station transmitter to preequalize the signal transmitted in the forward link. The error propagation of the DFE may result in channel information estimation errors. However, for slow fading channels, powerful tracking algorithms can be applied to suppress fast variation components in the channel estimation due to decision errors in the DFE and due to additive Gaussian noise, so that the estimation errors can be greatly reduced. In the system, most of the channel equalization function is performed in the base station, and the complexity of the portable unit can be greatly reduced.

With high-bit-rate transmission, the delay spread of the channel can be larger than the transmitted symbol interval T. The transmission channel is then modeled as a frequency-selective slow fading channel. The complex impulse response of the channel at the baseband for N_1 distinct propagation paths can be described as [19]–[21]

$$\tilde{h}(t) = \sum_{n=0}^{N_1-1} \tilde{\alpha}_n(t) e^{j\tilde{\phi}_n(t)} \delta(t - \tilde{\tau}_n(t)) \tag{1}$$

where $\tilde{\alpha}_n(t)$, $\tilde{\phi}_n(t)$, and $\tilde{\tau}_n(t)$ are the amplitude response, phase shift, and propagation delay for the nth path, respectively, and $\delta(t-\tilde{\tau}_n(t))$ is the impulse at $t = \tilde{\tau}_n(t)$. $\tilde{\alpha}_0(t)$ at any t is Rician distributed if there is a line-of-sight (LOS) path, and Rayleigh distributed otherwise. On the other hand, the amplitude response of the delayed paths $\tilde{\alpha}_n(t)(n > 0)$ is usually Rayleigh distributed with the phase response $\tilde{\phi}_n(t)$ uniformly distributed over [0, 2π]. For simplicity, assume $\tilde{\tau}_n(t) = nT$. As a result, the channel impulse response can further be simplified to

$$\tilde{h}(t) = \sum_{n=0}^{N_1-1} \tilde{h}_n(t) \delta(t - nT) \tag{2}$$

where $\tilde{h}_n(t) = \tilde{\alpha}_n(t) e^{j\tilde{\phi}_n(t)}$. For slow fading channels, we assume that $\tilde{\alpha}_n(t)$ and $\tilde{\phi}_n(t)$ are time-invariant over each frame.

With coherent detection, we can represent the wireless transmission system equivalently at baseband. Consider the baseband effective channel, which consists of the transmitter filter, the physical wireless channel, and the receiver matched filter. If we sample the output of the matched filter at the end of each symbol interval, the received symbol sequence $\{r_i\}$ is given by

$$r_i = \sum_{n=0}^{N_2-1} h_n x_{i-n} + \eta_i = h_0 x_i + I_i + \eta_i \tag{3}$$

where $N_2 \geq N_1$, $\{h_n\}$ is the sequence of coefficients of the equivalent discrete-time channel response, $h_0 x_i$ is the weighted ith transmitted symbol at the baseband (weighted by h_0), $I_i = \sum_{n=1}^{N_2-1} h_n x_{i-n}$ is the ISI, and $\{\eta_i\}$ is a discrete-time white Gaussian noise sequence.

III. Precoding With Small Envelope Variations

In the following, the new precoding schemes with small envelope variations are developed for $\pi/4$-QPSK and MSK based on the dimension partitioning concept. We first assume $h_0 = 1$ and then discuss the case when $h_0 \neq 1$. For completeness, the concept of dimension partitioning for precoding QPSK signals [14] is first reviewed.

A. Precoding for QPSK Using Dimension Partitioning

In (3), given $h_0 = 1$, if the desired received symbol (ISI and noise free) is d_i, then the transmitted symbol after precoding should be $x_i = d_i - I_i$. However, when the channel is not minimum phase, the amplitude of the transmitted symbol approaches infinity. To overcome the precoder instability, TH precoding for 2×2 quadrature amplitude modulation (QAM) generates the transmitted symbol $x_i' = d_i - I_i'$, where $I_i' = I_i - 2(u_i + jv_i)L$ is referred to as truncated ISI, $L/2$ is the magnitude of the real and imaginary parts of the 4-QAM symbols, and u_i and v_i are integers such that both the in-phase and quadrature components of the precoded symbol x_i' are in the range $[-L, +L]$. Truncating ISI from I_i to I_i' is done by modulo-$2L$ arithmetic operation to the in-phase and quadrature components of the ISI, respectively. At the receiver, the desired symbol is recovered from the received symbol by the same modulo arithmetic operation. The TH precoding predistorts the transmitted symbol amplitude to achieve both ISI-free transmission and the precoder stability via the modulo arithmetic operation.

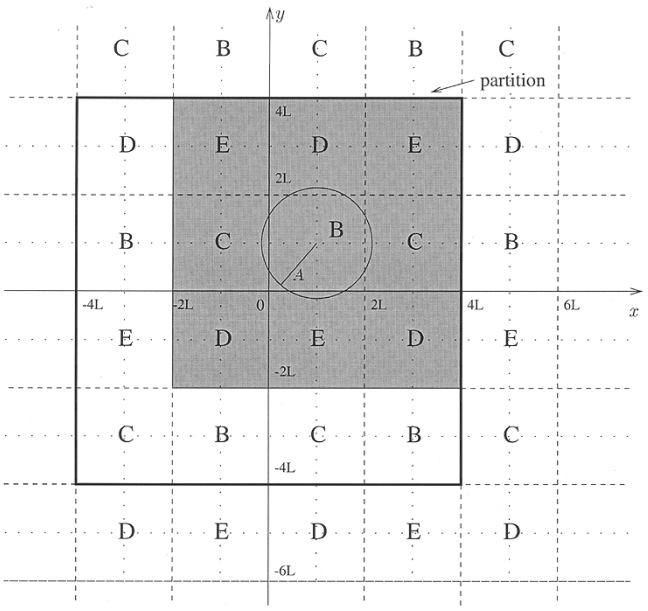

Fig. 2. The signal space partitioning for the QPSK precoding.

The precoding scheme for QPSK [14] is developed based on the TH precoding with some modifications. To achieve a constant transmitted symbol amplitude, denoted by A, in the two-dimensional (2-D) signal space, the precoded symbol should be on the circle centered at the truncated ISI with radius A. This circle is referred to as ISI circle. The precoder finds the best signal point (denoted by b_i for the ith symbol) on the circle, which corresponds to the minimum transmission error rate. To illustrate the process of finding the best signal point, the 2-D signal space of QPSK is partitioned into 16 square regions with sides $2L$, labeled with B, C, D, E (corresponding to the four information symbols in QPSK), as shown in Fig. 2. Regions with the same label represent the same 2-bit information symbol. The truncated ISI is always in the region B at the center (referred to as base region B). If $A \in [5L/4, \sqrt{2}L)$, the ISI circle always stays in the nine shaded regions and overlaps with the regions representing all four different phases of QPSK signals [22]. Correct detection can be achieved as long as the signal applied to the decision device lies in the correct decision region. The best signal point on the ISI circle is the one (in the region for the information symbol) that has the largest distance from the region boundaries. The output of the precoder is $x_i' = b_i - I_i'$.

The precoding for QPSK intends to limit envelope variations of the transmitted signal by keeping a constant transmitted symbol amplitude. However, it does not avoid the phase shifts of $\pm\pi$ rad between successive symbols, which can make the

envelope go to zero after filtering. Thus, the precoding process in discrete T-spaced moments without any constraint on the phase of precoded symbols can still have a large envelope variation from time to time, which may mean a substantial instantaneous bandwidth expansion after a power-efficient nonlinear amplifier. The bandwidth expansion is not desired in wireless communications as each user is allowed to transmit only in the strictly assigned frequency band.

B. Precoding for $\pi/4$-QPSK

The $\pi/4$-QPSK signal constellation consists of two QPSK signal constellations offset by $\pi/4$ relative to each other. The two signal constellations are used alternatively from symbol to symbol. At any symbol interval, a signal point is chosen from the QPSK constellation to represent the two information bits. The even-numbered symbols can have phases $\pm\pi/4$ and $\pm 3\pi/4$, whereas odd-numbered symbols can have phases 0, $\pm\pi/2$, and π. There are a total of eight possible signal points, and the phase change between any two consecutively transmitted QPSK symbols is limited to the set $\{\pi/4, 3\pi/4, 5\pi/4, 7\pi/4\}$. To represent the $\pi/4$ phase shift between the two QPSK constellations, let the four regions shown in Fig. 2 represent the phases $\pm\pi/4$ and $\pm 3\pi/4$ for even-numbered symbols and the phases 0, $\pm\pi/2$, and π for odd-numbered symbols. As a result, in the following discussion, we focus on one QPSK signal constellation to represent the four QPSK signals of either odd-numbered or even-numbered symbols.

1) Precoding: The first step in the precoding is to obtain the truncated ISI I_i' from the known channel information and the previously transmitted signals. According to the position of the ISI, the phase represented by each region is determined. The best signal point b_i on the ISI circle in the correct region is then determined, and the precoded symbol is the difference between the best signal point and the truncated ISI, i.e., $x_i' = b_i - I_i'$. The main issues in the precoding are how to define the meanings of the signal regions and how to find the best signal point b_i.

a) The signal regions: Due to the special arrangement of square regions in a partition, each region does not always represent the same phase of the transmitted symbols [14]. The actual ISI before truncation can lie in any region, but the truncated ISI can only lie in the base region B. Hence, the real ISI and the truncated ISI have different reference region patterns surrounding them. During precoding, the best signal point is on the ISI circle centered at the truncated ISI; however, the received signal is on the corresponding circle centered at the actual ISI. After the modulo arithmetic operation, the received signal may not be shifted to the region specified in the precoding procedure. For example, in Fig. 3, the actual ISI lies in region D and the desired signal point is in region C. At the receiver, the received signal r_i is truncated to $\hat{d}_i$ (after the modulo arithmetic operation), which lies in region B, as shown in Fig. 4. As a result, the meanings of the signal regions should be determined such that

1) no matter what the combination of (u_i, v_i) is, the pattern of B, C, D and E does not change;
2) the ISIs located in the regions with the same label have the same reference pattern surrounding them;
3) the phases represented by each partition of B, C, D, and E after the modulo operation are the same.

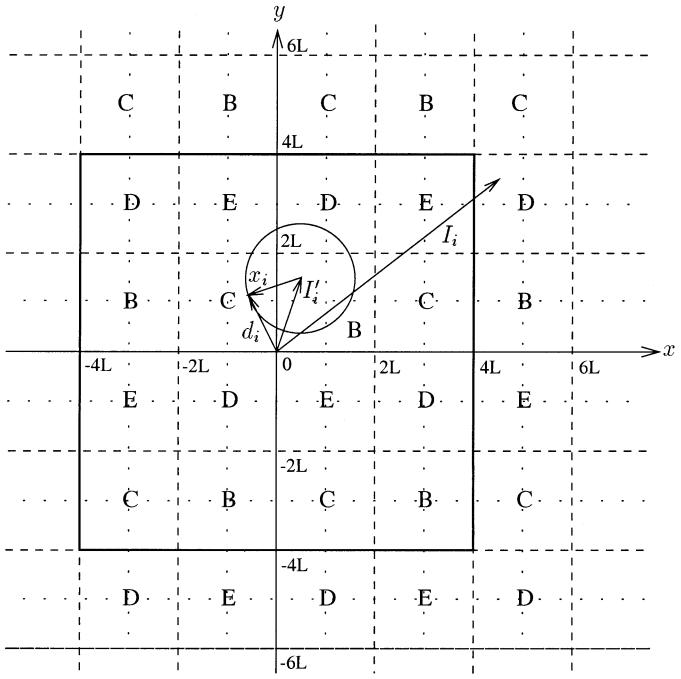

Fig. 3. An example of the precoding procedure for $\pi/4$-QPSK.

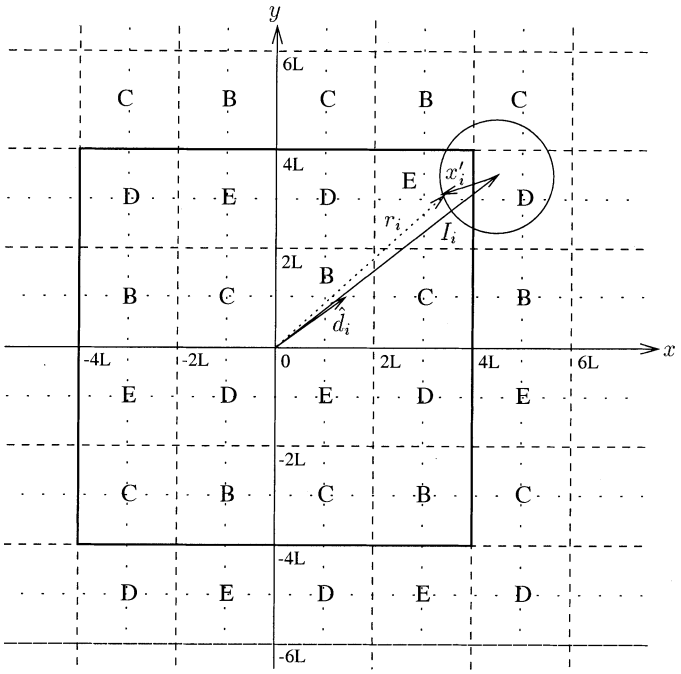

Fig. 4. An example of the decoding procedure for $\pi/4$-QPSK.

The relation between (u_i, v_i) and the phases represented by each region after the modulo operation is developed and illustrated in Fig. 5. As the pattern of the signal space partitioning is fixed (independent of the actual carrier phase of the original $\pi/4$-QPSK symbol), in finding the best signal point, cases of the desired phase in B, C, D, and E regions, respectively, are considered instead of their actual phases such as $\pi/4$, $3\pi/4$, etc.

b) The best signal point: The signal point must lie on the ISI circle to keep a constant transmitted symbol amplitude. In choosing a point from the ISI circle as the best signal point, two

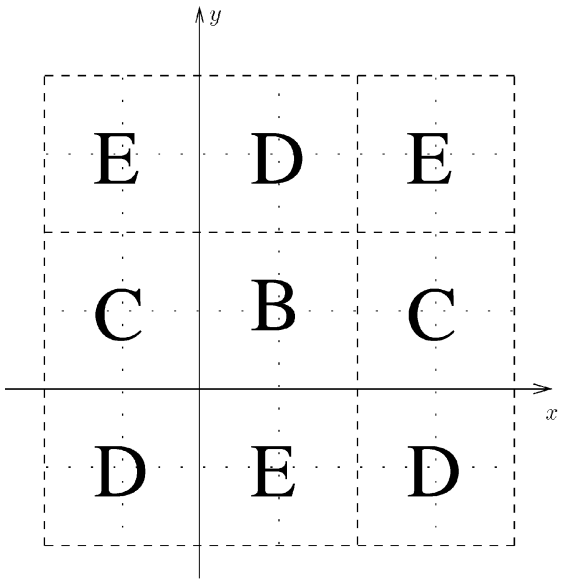

$(u_i \bmod 2, v_i \bmod 4) : B, C, D, E$

	odd-numbered; even-numbered symbols
$(0,0)$ or $(1,2) : 0, \pi/2, \pi, 3\pi/2$;	$\pi/4, 3\pi/4, 5\pi/4, 7\pi/4$
$(0,1)$ or $(1,3) : \pi, 3\pi/2, \pi/2, 0$;	$5\pi/4, 7\pi/4, 3\pi/4, \pi/4$
$(0,2)$ or $(1,0) : \pi/2, 0, 3\pi/2, \pi$;	$3\pi/4, \pi/4, 7\pi/4, 5\pi/4$
$(0,3)$ or $(1,1) : 3\pi/2, \pi, 0, \pi/2$;	$7\pi/4, 5\pi/4, \pi/4, 3\pi/4$

Fig. 5. Relationship between (u_i, v_i) and the region pattern for the $\pi/4$-QPSK precoding.

criteria are considered: transmission accuracy and carrier phase change between adjacent precoded symbols. The best signal point should give a low BER and, at the same time, should avoid a phase change close to or equal to $\pm\pi$ in order to reduce the envelope variation of the transmitted signal after filtering.

The transmission accuracy can be represented by the probability that the received signal lies outside the correct decision region. For easy calculation, the noise effect on the received signal is translated to that on the best signal point. The probability of the received signal's lying outside the correct decision region is equal to the probability of the additive Gaussian noise shifting the best signal point to another signal region. From Fig. 6, assuming that the probability of shifting the best signal to another region with the same label is very small, if the best signal point $b_i = (x, y)$ lies in region B, i.e., $x, y \in [0, 2L)$, the probability that the received signal lies outside the desired decision region is [14]

$$\begin{aligned} Q_B(x, y) = {} & Q\left(\frac{1}{\delta_\eta}x\right) + Q\left(\frac{1}{\delta_\eta}(2L-x)\right) + Q\left(\frac{1}{\delta_\eta}y\right) \\ & + Q\left(\frac{1}{\delta_\eta}(2L-y)\right) - Q\left(\frac{1}{\delta_\eta}x\right)Q\left(\frac{1}{\delta_\eta}y\right) \\ & - Q\left(\frac{1}{\delta_\eta}x\right)Q\left(\frac{1}{\delta_\eta}(2L-y)\right) \\ & - Q\left(\frac{1}{\delta_\eta}(2L-x)\right)Q\left(\frac{1}{\delta_\eta}y\right) \\ & - Q\left(\frac{1}{\delta_\eta}(2L-x)\right)Q\left(\frac{1}{\delta_\eta}(2L-y)\right) \end{aligned} \quad (4)$$

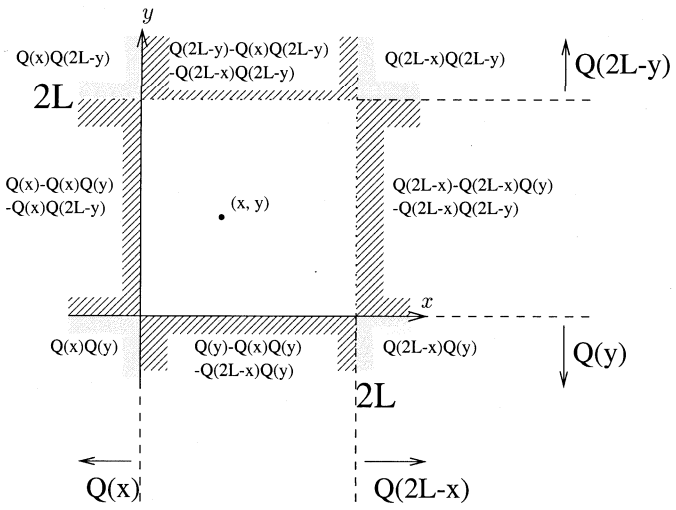

Fig. 6. Symbol error probability with the best signal point (x, y).

where $Q(x) = (1/\sqrt{2\pi})\int_x^\infty \exp(-(t^2/2))\,dt$ and δ_η is the standard deviation of the discrete additive Gaussian noise component (η_i) sampled at the output of the receiver matched filter. Similar calculations of the error probability can be done for other desired decision regions [23]. In general, the transmission accuracy measure function $\tilde{Q}_B(x, y)$ can be defined as

$$\tilde{Q}_B(x, y) = Q_B(x - 2pL, y - 2qL) \quad (5)$$

where p and q are some integers such that $x \in [2pL, (p+1)2L)$, $y \in [2qL, (q+1)2L)$. The smaller the value of $\tilde{Q}_B(x, y)$, the better the transmission accuracy.

Let $x_i' = A\exp(j\gamma_i)$ be the ith precoded symbol, and let $\Delta\gamma_i(=\gamma_i - \gamma_{i-1})$ be the phase change between the adjacent symbols. It is desired that the phase change should stay far away from π. Here, we define a phase change measure as

$$\Lambda_i = |(\Delta\gamma_i) \bmod [-\pi, +\pi]|. \quad (6)$$

The smaller the Λ_i value, the smaller the envelope variation and the better the precoder performance.

Taking into account both the transmission accuracy measure and the phase change measure, the final function for evaluating a signal point on the ISI circle Ψ for the ith symbol is defined as

$$\Psi_i = \tilde{Q}_B(x, y) * w + \Lambda_i \quad (7)$$

where w is the relative weighting factor of the transmission accuracy measure to the phase measure. To find the best signal point, the arc of the ISI circle in the desired decision region is divided into small segments. The number of segments increases with the length of the arc. The coordinates of the endpoints of each segment are substituted into (7). The point with the smallest value of the Ψ function is chosen as the best signal point. The best signal point is a function of the additive noise power of the received signal. As $Q(x)$ is a monotonically decreasing function of x and δ_η is simply a scaling factor in all the $Q(\cdot)$ functions in (4), the effect of δ_η on the value of Ψ in (7) and therefore the choice of the best signal point can be compensated, to a large extent, by a proper choice of the weighting factor w. Note that, without the phase change constraint, the precoder does not require the knowledge of the noise power [14].

As a result, in practical implementation, the estimation of the δ_η value can be avoided by using typical values of both δ_η and w for the target propagation environment. To achieve a smaller envelope variation, the best signal point may have a larger BER than the one without the phase shift measure. Even though the signal is precoded symbol by symbol, the phase change constraint will result in a smaller envelope fluctuation of the precoded signal as compared with the QPSK precoding in [14]. The reduced envelope variation is obtained at the cost of the transmission accuracy.

$\pi/4$-QPSK is proposed to achieve less envelope variations as compared with QPSK [18], in the absence of ISI. However, when precoding is used in the presence of ISI, the advantage of using $\pi/4$-QPSK would be reduced if no constraint on the phase change of the precoded symbols is considered. This is because the phase of the precoded symbol depends on the ISI and is therefore a random variable. The constraint on the phase change is essential to ensure small envelope fluctuations in the presence of ISI. When the ISI is not severe, the degree of the randomness in the precoded symbol phase is limited. Using $\pi/4$-QPSK indeed reduces envelope fluctuations even with precoding.

2) Decoding: After passing through the dispersive channel, the ith received symbol is

$$\begin{aligned} r_i &= x_i' + I_i + \eta_i \\ &= d_i + 2(u_i + jv_i)L + \eta_i. \end{aligned} \tag{8}$$

To recover the signal, the decoder at the receiver applies the same modulo-$2L$ arithmetic operation on the received signal. The signal after the modulo operation is

$$\hat{d}_i = r_i - 2(\hat{u}_i + j\hat{v}_i)L \tag{9}$$

for some integers $\hat{u}_i$ and $\hat{v}_i$ such that both the real and imaginary parts of $\hat{d}_i$ are in the range of $[-L, L]$. The decision device determines the phase represented by $\hat{d}_i$ depending on the $\hat{u}_i$ and $\hat{v}_i$ values, according to the relations shown in Fig. 5. When coded modulation is used to further improve the transmission accuracy, a Viterbi decoder should be implemented at the receiver after decoding the precoded signal. To combine demodulation with Viterbi decoding for better performance, the decoder of the precoded signal should not make a hard decision on the transmitted coded symbols. As a result, the Viterbi decoder input should include $\hat{d}_i$, in addition to $\hat{u}_i$ and $\hat{v}_i$. Even though how to map the value of $(\hat{d}_i, \hat{u}_i, \hat{v}_i)$ to the Viterbi decoding metrics needs further investigation, it is expected that the interconnection of the decoder for the precoding and the Viterbi decoder is straightforward, as the ISI component at the input of the Viterbi decoder has been significantly reduced (if not completely removed) by the precoding and decoding process prior to the Viterbi decoding.

In the example illustrated in Figs. 3 and 4, an even-numbered symbol with phase of $7\pi/4$ is transmitted, $(u_i, v_i) = (0, 1)$, and the truncated ISI locates in the left half of the region B. Hence, the best signal point is in the left region C. At the receiver, $(\hat{u}_i, \hat{v}_i) = (1, 1)$, and $\hat{d}_i$ lies in region B; therefore, the decoder will determine the signal phase as $7\pi/4$, which is a correct detection.

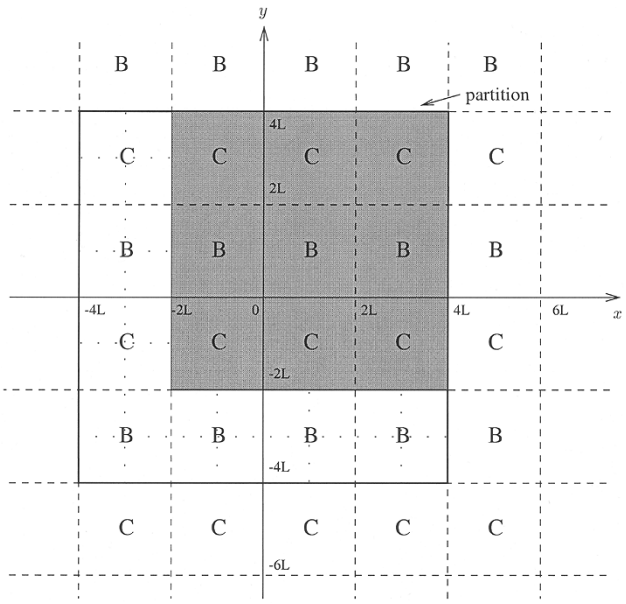

Fig. 7. The signal space partitioning for the MSK precoding.

C. Precoding for MSK

MSK is binary continuous-phase frequency-shift keying (CPFSK) with the modulation index $h = 1/2$. The phase continuity is maintained at any time instant to produce a constant envelope. The phase transition over a symbol interval depends on information transmitted, i.e., $\Delta\gamma_i = (\pi/2)m_i$, where $m_i = 1$ for symbol "1" and $m_i = -1$ for symbol "0." Due to the constraint of continuous phase, the signal constellation of MSK is similar to that of QPSK, even though MSK is a binary modulation scheme. In the MSK signal constellation, one of two message points is used to represent the transmitted symbol at any one time, depending on the initial phase for the symbol interval. In coherent detection of the MSK signal, the phases at the beginning and the end of the symbol interval are estimated, each based on the received signal waveform over the two-symbol interval, and then an estimate of $\Delta\gamma_i$, $\Delta\hat{\gamma}_i$, is obtained [24]. The receiver decides that a "1" was sent if $0 \le \hat{\Delta}\gamma_i \le \pi$, and "0" otherwise. To obtain correct detection, the estimated phase difference only needs to fall between 0 and π for symbol "1" and between 0 and $-\pi$ for symbol "0." For convenience, the phase reference is rotated by $\pi/2$ such that a phase difference between $-\pi/2$ and $\pi/2$ corresponds to symbol "1" and a phase change outside the range corresponds to symbol "0." Therefore, in precoding, the signal space is divided into partitions of two distinct regions, B and C, representing phases $+\pi/2$ and $-\pi/2$, respectively, as shown in Fig. 7. The ISI circle always stays in the shaded area and intersects the two regions.

Similar to the precoding for $\pi/4$-QPSK, the first step to precode the signal is to truncate the estimated ISI through the modulo operation such that both in-phase and quadrature components of the truncated ISI are in the range $[0, 2L]$. According to the position of the actual ISI, the decision region of the desired signal is determined. Since the region pattern repeats every two rows, if v_i is even, region B represents $\pi/2$ and region C represents $-\pi/2$, and vice versa otherwise. At each sampling moment, the point on the ISI circle with the lowest error probability is chosen as the best signal point. Between two sampling

moments, the phase of the precoded signal changes smoothly from one point to another to maintain the phase continuity, in order to keep the constant transmitted signal envelope as in MSK without precoding. The difference between the best signal point and the truncated ISI will be the precoded signal. Since the precoding scheme scrambles the precoded phase, $\Delta\gamma$ and h vary from symbol to symbol. As a result, the orthogonality between the original MSK signals no longer exists, and the precoded signal is a variant form of binary CPFSK. Note that the precoding for MSK is no longer T-spaced because the precoded signal has continuous phase and hence constant envelope.

As shown in Fig. 7, the signal space is partitioned only in the y-axis direction. As a result, the x-coordinate of the best signal point does not affect the transmission BER. The y-coordinate of the best signal point depends on the ISI and the transmission information symbol, which determines the decision region. If the decision region is B, the y-coordinate is

$$y = L. \tag{10}$$

Otherwise, if the decision region is chosen as C, the y-coordinate depends on the position of the ISI. Without loss of generality, assume $A = 1$. This requires that $L \in (\sqrt{2}/2,\ 4/5]$. The y-coordinate is

$$y = \begin{cases} -L, & \text{if } y_{I'} \in [0,\ 1-L) \\ y_{I'} - 1, & \text{if } y_{I'} \in [1-L,\ L) \\ y_{I'} + 1, & \text{if } y_{I'} \in [L,\ 3L-1) \\ 3L, & \text{if } y_{I'} \in [3L-1,\ 2L). \end{cases} \tag{11}$$

After passing through the multipath channel, the received symbol is detected by coherent demodulation. To recover the transmitted information symbol, the decoder at the demodulator applies the same modulo-$2L$ arithmetic operation on the received symbol such that both the real and imaginary parts of the symbol are in the range $[-L,\ L]$. If $\hat{v_i}$ is even, the decision device determines that the phase represented by $\hat{d_i}$ is $\pi/2$, and $-\pi/2$ otherwise. The phase difference between successive symbols is then found, and the transmitted information symbol is estimated.

D. First Path Fading Estimation

In developing the new precoding schemes, it is assumed that the first path of the multipath fading channel does not experience fading, i.e., $h_0 = 1$. However, the assumption is not valid in reality. For $h_0 = \alpha_0 e^{j\phi_0}$, the estimated ISI is normalized with respect to α_0 and the normalized ISI is used in the precoding scheme. Therefore, (4) corresponds to

$$\begin{aligned} Q_B(x,\ y) = & Q\left(\frac{\alpha_0}{\delta_\eta}\,x\right) + Q\left(\frac{\alpha_0}{\delta_\eta}\,(2L-x)\right) + Q\left(\frac{\alpha_0}{\delta_\eta}\,y\right) \\ & + Q\left(\frac{\alpha_0}{\delta_\eta}\,(2L-y)\right) - Q\left(\frac{\alpha_0}{\delta_\eta}\,x\right) Q\left(\frac{\alpha_0}{\delta_\eta}\,y\right) \\ & - Q\left(\frac{\alpha_0}{\delta_\eta}\,x\right) Q\left(\frac{\alpha_0}{\delta_\eta}\,(2L-y)\right) \\ & - Q\left(\frac{\alpha_0}{\delta_\eta}\,(2L-x)\right) Q\left(\frac{\alpha_0}{\delta_\eta}\,y\right) \\ & - Q\left(\frac{\alpha_0}{\delta_\eta}\,(2L-x)\right) Q\left(\frac{\alpha_0}{\delta_\eta}\,(2L-y)\right). \end{aligned} \tag{12}$$

Also, in order to counter the effect of the phase distortion, the precoded signal is multiplied by $e^{-j\phi_0}$ before being transmitted.

After passing through the multipath fading channel, the received signal is scaled by α_0. Therefore, a scaled decision region size and transmitted amplitude should be used in decoding, i.e., $2\alpha_0 L$ and $\alpha_0 A$ should be used instead of $2L$ and A. In a slow fading channel, α_0 remains approximately the same over a data frame. The value of α_0 can be estimated at the base station and then sent to the mobile receiver; or the base station can send a predefined training sequence of a few symbols for the receiver to estimate the α_0 value. The sequence should be designed in such a way that the symbols from the delayed paths cancel each other, which makes it possible to estimate the first-path amplitude fading α_0. As an example, consider a four-path channel, i.e., $N_2 = 4$ in (3). The received signal at the ith symbol interval is

$$r_i = \sum_{n=0}^{3} \alpha_n x'_{i-n} + \eta_i. \tag{13}$$

For $\pi/4$-QPSK, the symbol sequence $\{01,\ 00,\ 10,\ 00,\ 10,\ 11,\ 01,\ 00,\ 01,\ 11,\ 01,\ 11,\ 10\}$ can be chosen as the training sequence, corresponding to the phase sequence $\{\pi,\ 5\pi/4,\ 0,\ 5\pi/4,\ 0,\ \pi/4,\ \pi,\ 5\pi/4,\ \pi,\ \pi/4,\ \pi,\ \pi/4,\ 0\}$. Similarly, for MSK, the symbol sequence $\{1,\ 1,\ 1,\ 0,\ 1,\ 1,\ 1,\ 1,\ 0,\ 0,\ 1,\ 0,\ 0\}$ can be chosen as the training sequence, corresponding to the phase sequence $\{\pi/2,\ \pi,\ 3\pi/2,\ \pi,\ 3\pi/2,\ 0,\ \pi/2,\ \pi,\ \pi/2,\ 0,\ \pi/2,\ 0,\ 3\pi/2\}$ with the initial phase (for $i = 0$) being set at zero. As a result, the amplitude fading of the first path can be estimated as

$$\hat{\alpha_0} = \frac{|r_4 + r_8| + |r_7 + r_9| + |r_5 + r_{13}|}{6} \tag{14}$$

where $\hat{\alpha_0}$ follows a Gaussian distribution with mean $A\alpha_0$ and variance $\delta_\eta^2/3$. In general, for an N_2-path channel, we can obtain an estimated $\hat{\alpha_0}$, which is Gaussian distributed with mean $A\alpha_0$ and variance δ_η^2/l for $l \geq 2$, if a training sequence of $3l+N_2-1$ symbols is sent. The accuracy of the estimation increases with the length of the training sequence.

Since the effect of first path fading is cancelled at the receiver, the compensation factor $1/h_0$ can be avoided at the transmitter. As a result, the transmitted symbol amplitude can be kept constant even in the case that the main path experiences deep fading, and the precoder stability can be achieved.

IV. Theoretical Performance Analysis

Performance analysis of the newly proposed precoding schemes is carried out under the following assumptions.

1) The channel has two propagation paths ($N_2 = 2$) with the delay difference equal to T. The first path experiences Rician fading or Rayleigh fading, and the second path experiences Rayleigh fading.
2) The precoder has accurate channel information such that the estimated ISI is accurate.
3) The noise introduced by the channel is AWGN, and the message symbols are equiprobable.
4) The first path fading estimation at the receiver is accurate.

5) The transmitter has an accurate estimate of the additive noise power in the $\pi/4$-QPSK precoding, which is necessary to find the best signal point.

For a slow fading channel, the channel response is approximately time-invariant over one data frame. Therefore, $\alpha_0(t) \approx \alpha_0$, $\alpha_1(t) \approx \alpha_1$, $\phi_0(t) \approx \phi_0$, $\phi_1(t) \approx \phi_1$, where α_0, α_1, ϕ_0, and ϕ_1 are random variables. Then, the ith received symbol in the frame is

$$\begin{aligned} r_i &= \alpha_0 e^{j\phi_0} x'_i + \alpha_1 e^{j\phi_1} x'_{i-1} \\ &= A\left[\alpha_0 e^{j(\phi_0+\gamma_i)} + \alpha_1 e^{j(\phi_1+\gamma_{i-1})}\right]. \end{aligned} \tag{15}$$

Without loss of generality, assume $A = 1$ and $L \in (\sqrt{2}/2, 4/5]$. The ISI is $I_i = \alpha_1 e^{j(\phi_1+\gamma_{i-1})}$. Since ϕ_1 is uniformly distributed over [0, 2π] for the Rayleigh faded path, the combined phase $(\phi_1 + \gamma_{i-1})$ is also uniformly distributed over [0, 2π]. As α_1 is Rayleigh distributed, the ISI can be split into independent Gaussian distributed in-phase and quadrature components. If the portion of power carried by the second path is $2\delta_2^2$ (which is also the variance because of the zero mean), the probability density functions for the truncated ISI components, $X_{I'}$ and $Y_{I'}$, after modulo-arithmetic operation and normalizing the ISI with respect to the amplitude fading of the first path α_0 are

$$\begin{aligned} f_{X_{I'}|\alpha_0}(x_{I'}) &= \frac{\alpha_0}{\sqrt{2\pi}\delta_2} \sum_{u=-\infty}^{\infty} \exp\left[-\frac{\alpha_0^2(2uL + x_{I'}^2)}{2\delta_2^2}\right], \\ &\qquad x_{I'} \in [0,\, 2L) \\ f_{Y_{I'}|\alpha_0}(y_{I'}) &= \frac{\alpha_0}{\sqrt{2\pi}\delta_2} \sum_{v=-\infty}^{\infty} \exp\left[-\frac{\alpha_0^2(2vL + y_{I'}^2)}{2\delta_2^2}\right], \\ &\qquad y_{I'} \in [0,\, 2L). \end{aligned} \tag{16}$$

1) $\pi/4$-QPSK: Given the amplitude fading α_0 and the best signal point $b_i = (x, y)$, the conditional probability of error $P_{e|\alpha_0, x, y}$ can be calculated using the same approach as that given in [14]. The best signal point in general is a function of the truncated ISI (x'_I, y'_I). Let $x = f_1(x'_I, y'_I)$ and $y = f_2(x'_I, y'_I)$ denote the relation between the best signal point and the truncated ISI; then the probability of error is

$$\begin{aligned} P_e = \int_0^{\infty} \Bigg[\int_0^{2L} \int_0^{2L} & P_{e|\alpha_0, f_1, f_2} f_{X'_I|\alpha_0} \\ & \cdot (x'_I) f_{Y'_I|\alpha_0}(y'_I)\, dx'_I\, dy'_I \Bigg] f_R(\alpha_0)\, d\alpha_0 \end{aligned}$$

where $f_R(\cdot)$ is the probability density function of the first path amplitude fading. Because the best signal point is determined by the Q function and the phase shift, it is very difficult to obtain the functions $f_1(\cdot)$ and $f_2(\cdot)$ to analytically describe the relation between the best signal point and the truncated ISI. As a result, the exact probability of error is difficult to calculate. However, if we relax the constraint on the phase change between the adjacent precoded symbols and choose the best signal point simply based on the criterion of minimizing the probability of error, we obtain a lower bound of transmission error. The lower bound can be evaluated in the same way as that given in [14].

2) MSK: Correct detection is achieved if the absolute phases of the current symbol and previous symbol are correctly detected or if both the phases are incorrectly detected and the phase change is correct. Each information symbol "0" or "1" corresponds to an MSK symbol phase β_0 or β_1, where $\beta_0 = 0$ and $\beta_1 = \pi$ for an even-numbered symbol, and $\beta_0 = -\pi/2$ and $\beta_1 = \pi/2$ for an odd-number symbol, given that the initial symbol phase is zero. Let θ_i and $\hat{\theta}_i \in \{\beta_0, \beta_1\}$ be the correct absolute phase and detected absolute phase of the ith transmitted symbol, P_j be the conditional probability of $\hat{\theta}_i = \beta_j$, $j = 0$ or 1, given that $\theta_i = \beta_0$. It can be shown [23] that the probability of correct detection P_c is $P_c = P_0^2 + P_1^2$. Different from $\pi/4$-QPSK, the coordinates of the best signal point can be expressed as functions of the truncated ISI, as given in (11) and (12). Therefore, the exact value of the error probability can be calculated. Given α_0 and the truncated ISI $(x_{I'}, y_{I'})$, the conditional probability of correct detection is

$$P_{c|\alpha_0, (x_{I'}, y_{I'})} = P^2_{0|\alpha_0, (x_{I'}, y_{I'})} + P^2_{1|\alpha_0, (x_{I'}, y_{I'})}. \tag{17}$$

The conditional probabilities are independent of $x_{I'}$, as the x-coordinate does not affect the detection decision in the proposed precoding. β_0 can be represented by decision region B or C. If both cases are equally likely, from (17), the conditional probability of error can be expressed as

$$\begin{aligned} P_{e|\alpha_0, y_{I'}} = 1 - \tfrac{1}{4} \Big[& \left(P_{1|B, \alpha_0, y_{I'}} + P_{1|C, \alpha_0, y_{I'}}\right)^2 \\ & + \left(P_{0|B, \alpha_0, y_{I'}} + P_{0|C, \alpha_0, y_{I'}}\right)^2 \Big]. \end{aligned} \tag{18}$$

For a given best signal point (x, y), $x, y \in [0, 2L)$, the probability of wrong detection is

$$\begin{aligned} Q_M(y) \approx & Q\left(\frac{\alpha_0}{\delta_\eta}(2L - y)\right) - Q\left(\frac{\alpha_0}{\delta_\eta}(4L - y)\right) \\ & + Q\left(\frac{\alpha_0}{\delta_\eta}(6L - y)\right) - Q\left(\frac{\alpha_0}{\delta_\eta}(8L - y)\right) \\ & + Q\left(\frac{\alpha_0}{\delta_\eta}(y)\right) - Q\left(\frac{\alpha_0}{\delta_\eta}(2L + y)\right) \\ & + Q\left(\frac{\alpha_0}{\delta_\eta}(4L + y)\right) - Q\left(\frac{\alpha_0}{\delta_\eta}(6L + y)\right). \end{aligned} \tag{19}$$

Given that the decision region is B and given α_0, from (10), the conditional probability of error is

$$P_{1|B, \alpha_0} = Q_M(L). \tag{20}$$

On the other hand, given decision region C, α_0, and the position of the truncated ISI, from (11), the error probability is given by

$$P_{1|C, \alpha_0, y_{I'}} = \begin{cases} Q_M(L), & \text{if } y_{I'} \in [0,\, 1 - L) \\ Q_M(y_{I'} - 1 + 2L), & \text{if } y_{I'} \in [1 - L,\, L) \\ Q_M(y_{I'} + 1 - 2L), & \text{if } y_{I'} \in [L,\, 3L - 1) \\ Q_M(L), & \text{if } y_{I'} \in [3L - 1,\, 2L). \end{cases} \tag{21}$$

As a result, given α_0, the error probability is

$$\begin{aligned}P_{e|\alpha_0} = &\int_0^{1-L}\Big\{1-\tfrac{1}{4}\Big[\big(P_{1|B,\alpha_0}+P_{1|C,\alpha_0,y_{I'}\in[0,1-L)}\big)^2\\&+\big(P_{0|B,\alpha_0}+P_{0|C,\alpha_0,y_{I'}\in[0,1-L)}\big)^2\Big]\Big\}f_{Y_{I'}|\alpha_0}(y_{I'})\,dy_{I'}\\&+\int_{1-L}^{L}\Big\{1-\Big[\tfrac{1}{4}\big(P_{1|B,\alpha_0}+P_{1|C,\alpha_0,y_{I'}\in[1-L,L)}\big)^2\\&+\big(P_{0|B,\alpha_0}+P_{0|C,\alpha_0,y_{I'}\in[1-L,L)}\big)^2\Big]\Big\}f_{Y_{I'}|\alpha_0}(y_{I'})\,dy_{I'}\\&+\int_{L}^{3L-1}\Big\{1-\Big[\tfrac{1}{4}\big(P_{1|B,\alpha_0}+P_{1|C,\alpha_0,y_{I'}\in[L,3L-1)}\big)^2\\&+\big(P_{0|B,\alpha_0}+P_{0|C,\alpha_0,y_{I'}\in[L,3L-1)}\big)^2\Big]\Big\}f_{Y_{I'}|\alpha_0}(y_{I'})\,dy_{I'}\\&+\int_{3L-1}^{2L}\Big\{1-\Big[\tfrac{1}{4}\big(P_{1|B,\alpha_0}+P_{1|C,\alpha_0,y_{I'}\in[3L-1,2L)}\big)^2\\&+\big(P_{0|B,\alpha_0}+P_{0|C,\alpha_0,y_{I'}\in[3L-1,2L)}\big)^2\Big]\Big\}f_{Y_{I'}|\alpha_0}(y_{I'})dy_{I'}\end{aligned}\tag{22}$$

where

$$\begin{aligned}P_{0|B,\,\alpha_0} &= 1-P_{1|B,\,\alpha_0}\\P_{0|C,\,\alpha_0,\,y_{I'}} &= 1-P_{1|C,\,\alpha_0,\,y_{I'}}.\end{aligned}$$

Finally, the error probability is

$$P_e=\int_0^{\infty}P_{e|\alpha_0}f_R(\alpha_0)\,d\alpha_0.\tag{23}$$

V. Numerical Results and Discussion

This section presents the performance of the newly proposed precoding schemes based on the theoretical analysis given in Section IV and based on computer simulation. As the precoded MSK signal has a constant envelope, the main performance measures of interest are BER for both $\pi/4$-QPSK and MSK and envelope variations for $\pi/4$-QPSK with bandpass filtering. In the simulation, the same assumptions as those in performance analysis are made, unless otherwise stated. The BER performance is evaluated for various values of the k factor of the first path Rician fading, defined as the ratio of the average power carried by the LOS component to that carried by the diffused component of the first path, and various values of the received signal-to-noise ratio per bit γ_b, defined as the ratio of the ensemble average of the received signal power per bit from both paths to the variance of the input Gaussian noise. The average power carried by the diffused component of the first path and that of the second path are assumed to be the same. The transmitted signal amplitude A is one and the precoding parameter L is 0.75. The value of γ_b is changed by changing the variance of the additive zero-mean Gaussian noise component. The relative weighting factor $w = 16$ is used. The diffusive component with Rayleigh distributed amplitude fading is simulated using the "sum of sine waves" method [25]. The Rician fading of the first path is simulated by adding a time-invariant LOS component to a Rayleigh distributed diffusive component. It is assumed that both the precoder and the DFE have accurate channel information, except when we investigate the effect of first path estimation error on the performance of the precoded system.

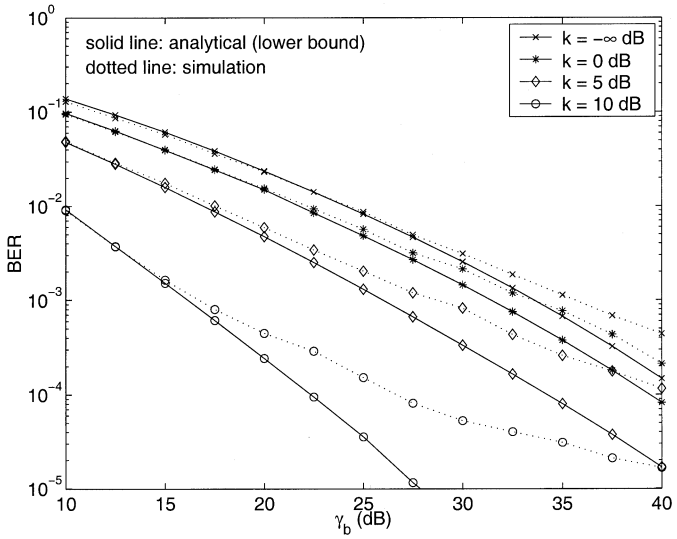

Fig. 8. Simulation results and analytical lower bounds for BER of $\pi/4$-QPSK using the precoder.

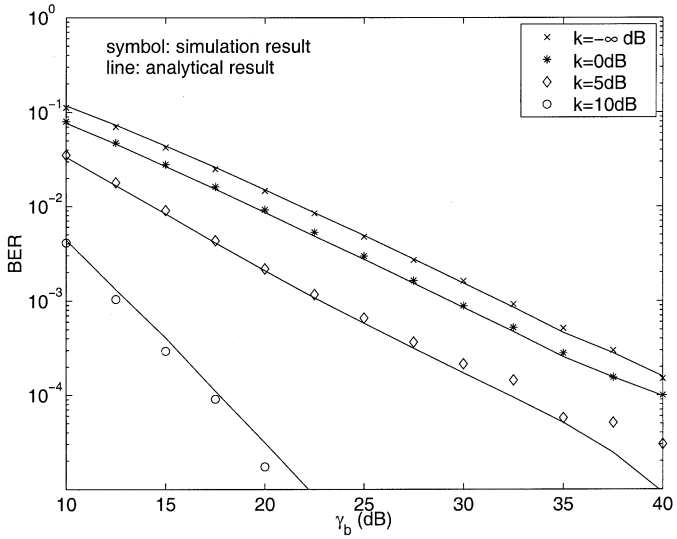

Fig. 9. Simulation and analytical results for BER of MSK using the precoder.

A. Effects of the k-Factor

Figs. 8 and 9 show BER versus γ_b for $\pi/4$-QPSK and MSK, respectively, using the precoding schemes when the k value varies. Both the analytical BER and the corresponding simulation results are given. The following observations can be made.

1) For MSK, the analytical results match well with the simulation results. For $\pi/4$-QPSK, the simulation results deviate from the analytical lower bound as γ_b increases. The

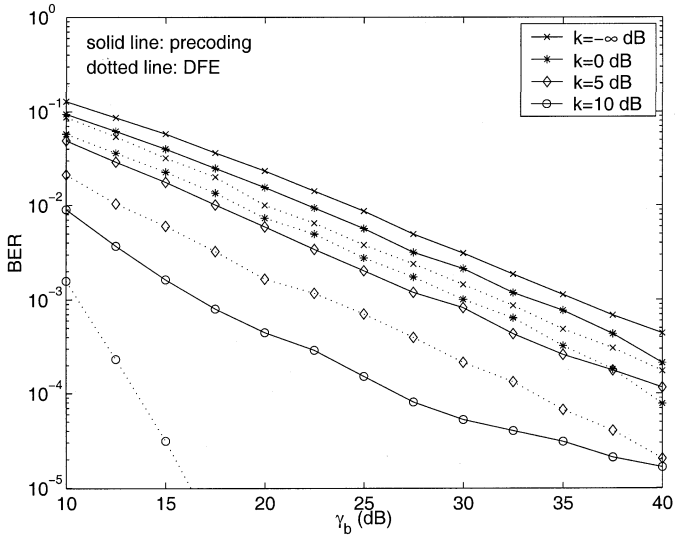

Fig. 10. Simulation results for BER of $\pi/4$-QPSK using the precoder and DFE, respectively.

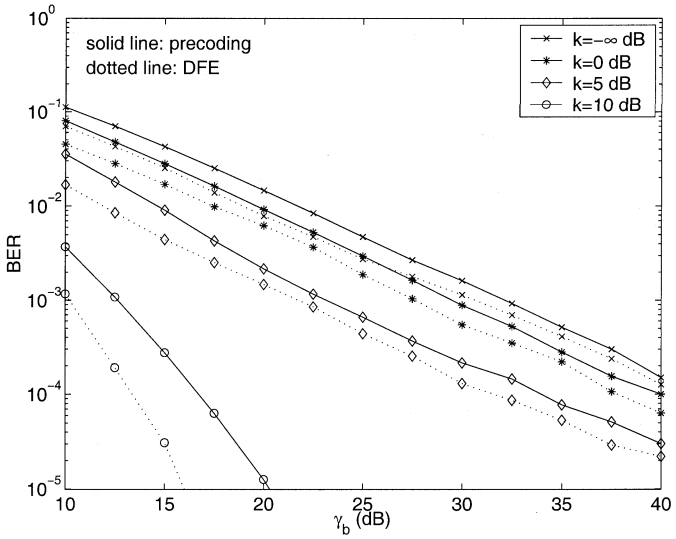

Fig. 11. Simulation results for BER of MSK using the precoder and DFE, respectively.

difference between the analytical bounds and the simulation results is caused by the phase change constraint imposed in the precoding. As a result, the effect of the phase change constraint on degrading the transmission accuracy increases when the effect of the channel additive Gaussian noise decreases.

2) When k increases from $-\infty$ to 0 dB, the performance improves only slightly. This is because the first path undergoes deep fading at a small k value. The reduced decision regions with side of $2\alpha_0 L$ in the precoding are very small, and the noise effect becomes significant.
3) When k increases from 5 to 10 dB, the performance is improved significantly. At a large k value, it is unlikely for the first path to experience deep fading. The decision regions are larger so that the effect of noise is reduced.
4) The phase change constraint in the precoding results in an error floor for $\pi/4$-QPSK at $k = 10$ dB.

B. Comparison With DFE

Consider a DFE consisting of a three-tap feedforward filter and a two-tap feedback filter. For a fair comparison, the DFE tap coefficients are always adjusted to their optimal values under the assumption that the receiver has accurate channel information. Figs. 10 and 11 show the computer simulation results of the BER performance when using the DFE for $\pi/4$-QPSK and MSK, respectively. For comparison, the corresponding BER curves when using the precoder are also plotted in the figures. The following can be observed.

1) The DFE outperforms the precoders, especially at a large K value (such as $k = 10$ dB), because the reduced decision regions and the phase change constraint in the precoding severely degrade the performance of the precoders.
2) At a small k value, the performance improvement of the DFE over the precoder is not significant, mainly due to the error propagation problem of the DFE. When the channel undergoes deep fading, the decision device is likely to make bursts of decision errors. As k increases, the constant component of the first path gets stronger and the noise effect is reduced.

If the accurate channel information is available to the DFE and if the transmission system does not employ channel coding, using the DFE at the portable unit receiver should be preferred to using the precoder, as the better transmission accuracy can be obtained without a significant increase of the receiver complexity. However, with channel coding, if the functions of the DFE and the Viterbi decoder are decoupled at the receiver for implementation simplicity, the transmission accuracy can be deteriorated significantly due to the unreliable zero-delay decisions (required by the DFE) in Viterbi decoder and due to the inherent error propagation of the DFE. As a result, with channel coding and Viterbi decoding, the precoder is expected to be a preferred choice if the receiver complexity is a main concern. Further research is necessary to investigate the tradeoff between the receiver complexity and the transmission accuracy.

C. Effect of First Path Estimation Error at the Receiver

Fig. 12 shows the BER performance when the receiver estimates the first path amplitude fading $\hat{\alpha_0}$ from a training sequence of length $l = 4, 19, 37, 162$, and ∞ (i.e., no estimation error), respectively, for both precoded MSK and $\pi/4$-QPSK in a Rayleigh fading environment ($k = -\infty$ dB), under the assumption that the first path phase distortion ϕ_0 is accurately estimated and compensated for at the base-station transmitter. It is observed that

1) as expected, the longer the training sequence, the better the BER performance with the more accurate estimation of the first path fading;
2) for the same training sequence length, the estimation error has more impact on the BER performance as γ_b increases.

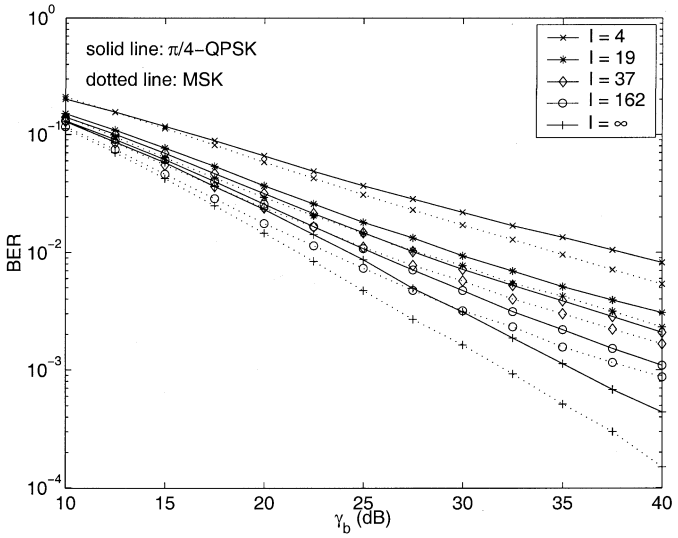

Fig. 12. BER when using precoders and the estimated $\hat{\alpha_0}$ at the receiver from the training sequences of different lengths for $k = -\infty$ dB.

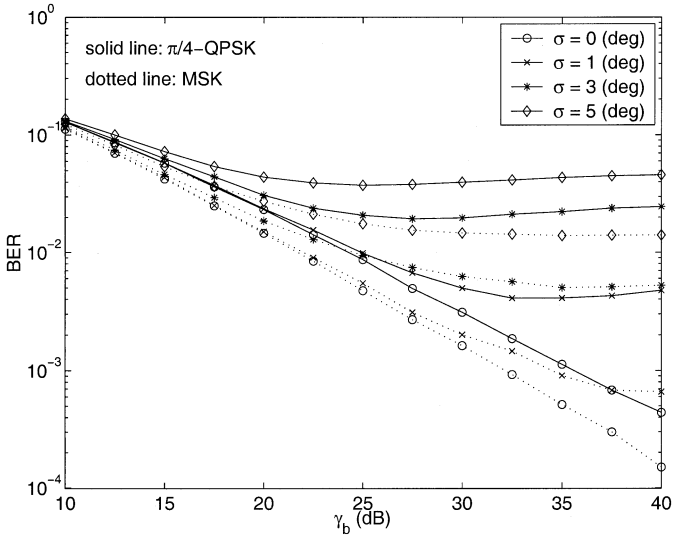

Fig. 13. BER for $k = -\infty$ dB when using precoders and the estimation error of ϕ_0 is Gaussian distributed with zero mean and standard deviation σ.

At a large γ_b value, the effect of noise is relatively minor and the first path estimation error has a dominant effect on the BER degradation.

Fig. 13 shows the BER performance with accurate estimate of the first path amplitude fading for both $\pi/4$-QPSK and MSK at $k = -\infty$ dB, under the assumption that the first path phase distortion ϕ_0 is estimated (at the base-station transmitter) with an error that is Gaussian distributed with zero mean and standard deviation (σ) of 1°, 3°, and 5°, respectively. For comparison, the results with an accurate ϕ_0 estimation are also given in the figure. It is observed that the precoding schemes are quite sensitive to the phase estimation error. In particular, the estimation error leads to a BER floor. As γ_b increases to a certain value, further increase of γ_b may actually increase BER when there is a phase estimation error. This is because the best signal point of the precoding schemes needs to meet the phase change constraints. At a large γ_b, the phase change constraint is the dominant factor in determining the best signal point, and a point very close to the decision region boundaries can be chosen (as the additive noise component is very small). In this case, a small phase estimation error is very likely to result in a signal detection error.

TABLE I
ENVELOPE VARIATIONS (IN dB) OF $\pi/4$-QPSK WITH SQUARE-ROOT RAISED COSINE FILTERING

α_{rf}	**standard $\pi/4$-QPSK**	**precoded $\pi/4$-QPSK**
0.35	-10.9	-13.8
0.5	-11.1	-14.1
0.7	-11.2	-14.3

D. Envelope Variations of $\pi/4$-QPSK

To study the envelope variations, we generate the transmitted signal after the transmitter filter by simulating the transmitter equivalently at baseband using Matlab Simulink software package. The in-phase and quadrature components of the transmitted symbol are first converted to two T-spaced rectangular waveforms, respectively. Each of the waveforms is first applied to a 1/sinc filter for sinc compensation and then applied to a square-root raised-cosine filter for the baseband pulse shaping [26], with the rolloff factors α_{rf} being 0.35, 0.5, and 0.7, respectively. The filtered in-phase and quadrature components are sampled, and the sampling interval is 1/10 of the symbol interval. Let $\tilde{x}_{j_I}$ and $\tilde{x}_{j_Q}$ denote the jth sampled in-phase and quadrature components after filtering, respectively. The envelope of the jth sample is $\varepsilon_j = \sqrt{\tilde{x}_{j_I}^2 + \tilde{x}_{j_Q}^2}$. The average envelope magnitude is always normalized to one, and the envelope variation V_ε is defined as

$$V_\varepsilon \triangleq 10 \times \log_{10} \left(\frac{\sum_{j=1}^{J} (\varepsilon_j - 1)^2}{J} \right) \quad (24)$$

in dB, where J is the number of samples.

Table I gives the envelope variations in dB of 1) filtered standard $\pi/4$-QPSK signal and 2) filtered $\pi/4$-QPSK precoded signal over the two-path channel with $k = 0$ dB and $\gamma_b = 40$ dB. The envelope variations of the precoded $\pi/4$-QPSK signal are smaller than those of the standard $\pi/4$-QPSK signal. During the simulation, it is observed that the probability of the phase change close to (but not equal to) π in the precoding decreases as γ_b increases. For example, at $k = 0$ dB, the probability of the phase change in $[3\pi/4, 5\pi/4]$ deceases from 0.19 at $\gamma_b = 10$ dB to 0.04 at $\gamma_b = 40$ dB. On the other hand, in the standard $\pi/4$-QPSK, both the phase changes of $3\pi/4$ and $5\pi/4$ always have a probability of 0.25 to occur. The phase change constraint, with $w = 16$ in (7), in the precoding indeed reduces the envelope fluctuations.

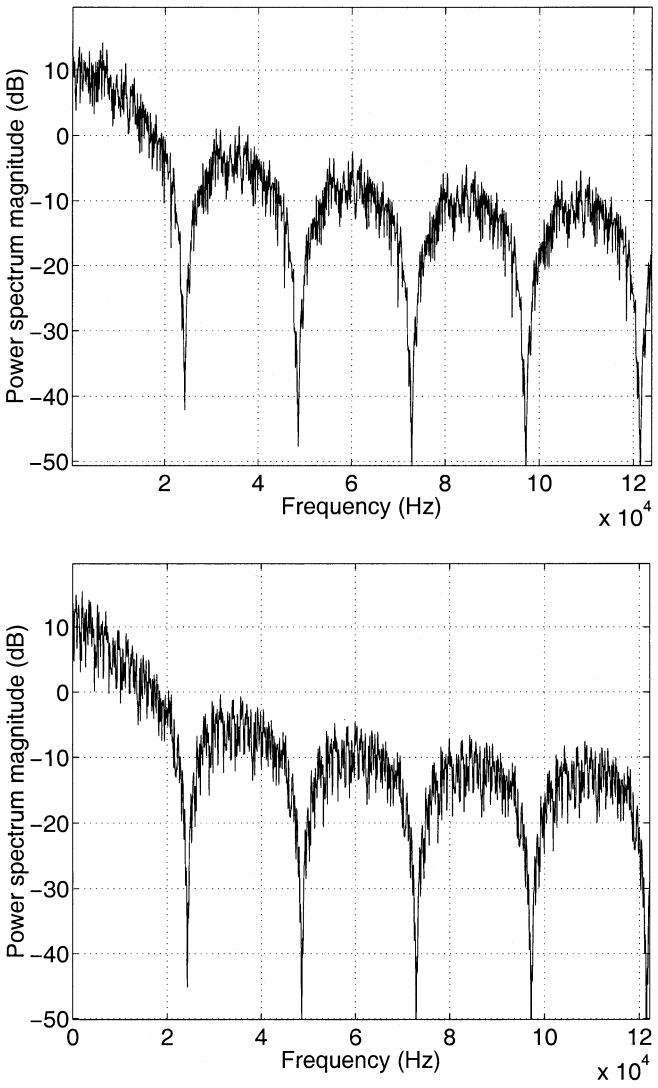

Fig. 14. Power spectral density of the $\pi/4$-QPSK signals (at baseband) without the filtering, with transmission rate of 2.43×10^4 symbols/s.

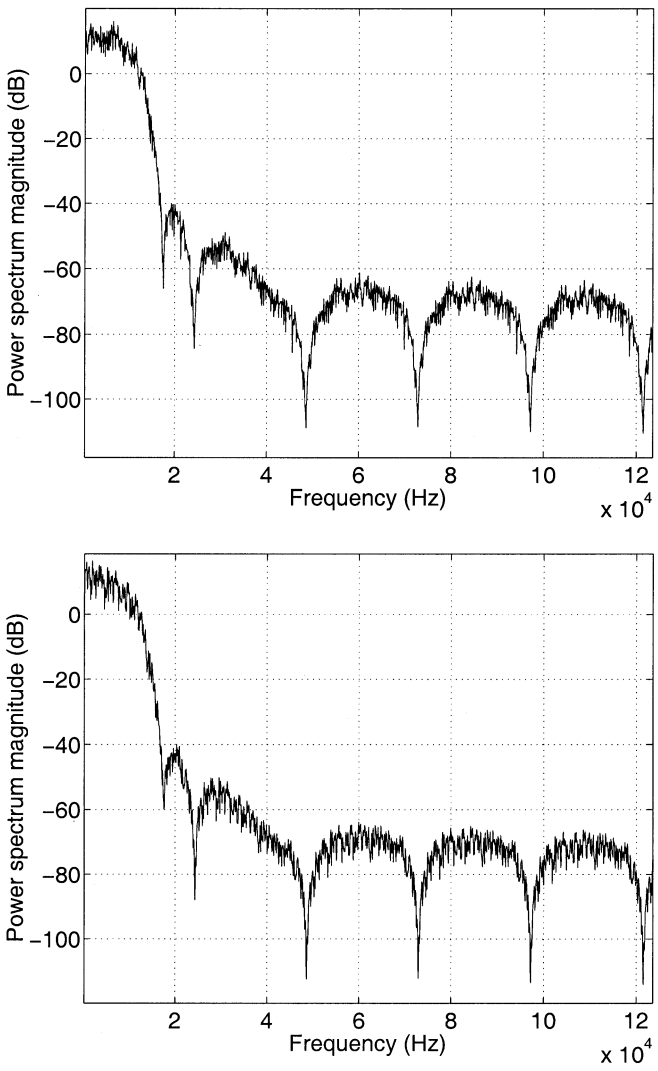

Fig. 15. Power spectral density of the $\pi/4$-QPSK signals (at baseband) after the square-root raised cosine filtering with the rolloff factor $\alpha_{rf} = 0.35$, with transmission rate of 2.43×10^4 symbols/s.

Figs. 14 and 15 plot the power spectral density (PSD) of the standard $\pi/4$-QPSK and precoded $\pi/4$-QPSK signals without filtering and with the square-root raised cosine filter at $\alpha_{rf} = 0.35$, respectively, where $k = 0$ dB, $\gamma_b = 40$ dB, and the symbol interval is $T = 4.116 \times 10^{-5}$ s, corresponding to a transmission symbol rate of 2.43×10^4 symbols/s. It is observed that the PSD of the precoded $\pi/4$-QPSK signal is very close to that of the standard $\pi/4$-QPSK signal, except that the side lobes of the precoded signal are slightly lower than those of the standard signal. With the filtering, from Fig. 15 and the power spectral densities for $\alpha_{rf} = 0.5$ and 0.7, it is observed that, as α_{rf} decreases, the bandwidth cutoff edge becomes shaper and the main lobe is more severely distorted. Consequently, envelope fluctuations increase as the rolloff factor decreases. As the precoder suppresses the side lobes of the PSD, the envelope variations of the precoded signals remain limited even though the side lobes are removed by the square-root raised cosine filters. Extensive simulation/experiment on the PSD of the precoded signals should be carried out for various fading environments, as the PSD depends on the channel fading and time dispersion conditions.

VI. Conclusion

Two new precoding schemes, one with small envelope variations for $\pi/4$-QPSK and the other with constant envelope for MSK, have been developed for frequency-selective slow fading channels, such as in indoor wireless communications. The precoding schemes are intended to be used in high-rate TDMA/TDD radio systems where ISI degrades transmission performance significantly. Under the condition that the channel fades slowly, the estimated channel information obtained from the receiver in the reverse link is used to perform signal precoding in the transmitter in the forward link. Based on the concept of signal space dimension partitioning, the precoders predistort only the phase of the transmitted symbol and keep the transmitted symbol amplitude constant. To achieve small envelope variations, phase shifts between successive symbols are limited. In $\pi/4$-QPSK precoding, BER is sacrificed to avoid

the phase changes close to or equal to $\pm\pi$. In MSK precoding, phase continuity is maintained at any time moment to maintain a constant envelope. The advantages of using the proposed precoding schemes are that

1) the effect of channel propagation time dispersion on transmission accuracy degradation is reduced without increasing the complexity of the portable unit receiver;
2) stability of precoders can be ensured even in preequalizing a nonminimum-phase fading channel;
3) envelope variations of transmitted signals are small in the $\pi/4$-QPSK precoding and are eliminated in the MSK precoding, and the use of a power-efficient nonlinear amplifier does not introduce significant nonlinear distortion.

To continue this research, channel coding should be considered. Powerful coded modulation techniques with a Viterbi decoder can be combined directly with the precoding to further improve the system performance [8], [9]. This can be achieved without a significant complexity increase of the portable unit, as the channel equalization function is decoupled from the Viterbi decoding process at the receiver. With channel coding, the tradeoff on transmission accuracy and system complexity between the precoding system and the DFE system needs further investigation.

ACKNOWLEDGMENT

The authors wish to thank the anonymous reviewers for their thorough reviews and helpful suggestions.

REFERENCES

[1] A. A. R. Townsend, *Digital Line-of-Sight Radio Links*. New York: Prentice-Hall, 1988.
[2] J. G. Proakis, *Digital Communications*, 2nd ed. New York: McGraw-Hill, 1989.
[3] E. Dahlman, "Adaptive decision-feedback equalizers for fast-varying mobile-radio channels," TRITA-TTT-8912, Dec. 5, 1989.
[4] S. U. H. Qureshi, "Adaptive equalization," *Proc. IEEE*, vol. 73, pp. 1349–1387, Sept. 1985.
[5] M. V. Eyuboglu and S. H. Qureshi, "Reduced-state sequence for coded modulation on intersymbol interference channels," *IEEE J. Select. Areas Commun.*, vol. 7, pp. 989–995, Aug. 1989.
[6] K. Wesolowski, "Efficient digital receiver structure for trellis-coded signals transmitted through channels with intersymbol interference," *Electron. Lett.*, vol. 23, no. 24, pp. 1265–1266, Nov. 1987.
[7] R. Benjamin, I. Kaya, and A. Nix, "Smart base stations for dumb time-division duplex terminals," *IEEE Commun. Mag.*, pp. 124–131, Feb. 1999.
[8] M. V. Eyuboglu and G. D. Forney, Jr., "Trellis precoding: Combined coding, precoding and shaping for intersymbol interference channels," *IEEE Trans. Inform. Theory*, vol. 38, pp. 301–314, Mar. 1992.
[9] K. Sripimanwat, H. Weinrichter, R. M. A. P. Rajatheva, and K. Ahmed, "Soft-detection phase precoding with MPSK-TCM for ISI channel," *IEEE Commun. Lett.*, vol. 5, pp. 163–165, Apr. 2000.
[10] M. Tomlinson, "New automatic equalizer employing modulo-arithmetic," *Electron. Lett.*, vol. 7, pp. 138–139, Mar. 1971.
[11] H. Harashima and H. Miyakawa, "Matched-transmission technique for channels with intersymbol interference," *IEEE Trans. Commun.*, vol. C-20, pp. 774–780, Aug. 1972.
[12] W. Zhuang, W. A. Krzymien, and P. A. Goud, "Adaptive channel precoding for slowly fading channels," in *Proc. PIMRC'94*, The Hague, The Netherlands, Sept. 18–23, 1994, pp. 660–664.
[13] W. Zhuang and W. V. Huang, "Phase precoding for frequency-selective Rayleigh and Rician slowly fading channel," *IEEE Trans. Veh. Technol.*, vol. 46, pp. 129–142, Feb. 1997.
[14] Y. Chan and W. Zhuang, "Channel precoding for indoor radio communications using dimension partitioning," *IEEE Trans. Veh. Technol.*, vol. 48, pp. 98–114, Jan. 1999.
[15] S. N. Crozier, "Precompensated frequency modulation (PFM) designed for $\pi/4$-shifted QPSK receivers," in *Proc. 18th Biennial Symp. Communications*. Kingston, Canada: Queens Univ., 1996, pp. 344–346.
[16] M. A. Low and P. H. Wittke, "Precoded nonlinear constant-envelope modulations," in *Proc. ISSSE'98*, 1998, pp. 349–355.
[17] *Interim Standard: Cellular System Dual-Mode Mobile Station—Base Station Compatibility Standard (IS-54)*, May 1990.
[18] Y. Akaiwa and Y. Nagata, "Highly efficient digital mobile communications with a linear modulation method," *IEEE J. Select. Areas Commun.*, vol. SAC-5, pp. 890–895, June 1987.
[19] A. A. M. Saleh and R. A. Valenzuela, "A statistical model for indoor multipath propagation," *IEEE J. Select. Areas Commun.*, vol. SAC-5, pp. 128–137, Feb. 1987.
[20] H. Suzuki, "A statistical model for urban radio propagation," *IEEE Trans. Commun.*, vol. COM-25, pp. 673–680, July 1977.
[21] H. Hashemi, "The indoor radio propagation channel," *Proc. IEEE*, vol. 81, pp. 943–967, July 1993.
[22] Y.-L. Chan, "Channel precoding with constant amplitude for QPSK over slowly fading channels using dimension partitioning technique," M.A.Sc. thesis, Dept. of Electrical and Computer Engineering, Univ. of Waterloo, May 1996.
[23] J. S. Y. Lee, "Channel precoding with small envelope variations for $\pi/4$-QPSK and MSK over frequency-selective slow fading channels," M.A.Sc. thesis, Dept. of Electrical and Computer Engineering, Univ. of Waterloo, May 2000.
[24] S. Haykin, *Communication Systems*, 4th ed. New York: Wiley, 2001.
[25] W. C. Jakes, Ed., *Microwave Mobile Communications*. New York: Wiley, 1974.
[26] W. Wang, *Communications Toolbox: For Use With Matlab*: The MathWorks Inc., 1996.

Jennifer S. Y. Lee was born in Hong Kong, China, on September 4, 1973. She received the B.Sc. and M.Sc. degrees in electrical and computer engineering from the University of Waterloo, Waterloo, ON, Canada, in 1998 and 2000, respectively.

She is currently a Software Developer with Kaval Wireless Technologies Inc., working on a remote management system for wireless coverage extension system.

Weihua Zhuang (M'93–SM'01) received the B.Sc. and M.Sc. degrees from Dalian Marine University, China, in 1982 and 1985, respectively, and the Ph.D. degree from the University of New Brunswick, Canada, in 1993, all in electrical engineering.

Since October 1993, she has been with the Department of Electrical and Computer Engineering, University of Waterloo, ON, Canada, where she is a Professor. She is a coauthor of *Wireless Communications and Networking* (Englewood Cliffs, NJ: Prentice-Hall, 2002). Her current research interests include multimedia wireless communications, wireless networks, and radio positioning.

Dr. Zhuang is a Licensed Professional Engineer in the Province of Ontario, Canada. She received the Premier's Research Excellence Award (PREA) from the Ontario Government in 2001.